Interaction of Divalent Cations with Germ Cell Specific Sulfogalactosylglycerolipid and the Effects on Lipid Chain Dynamics†

Susanne Tupper,‡ Patrick T. T. Wong,§ Morris Kates,|| and Nongnuj Tanphaichitr*,‡

Human IVF Labs, Reproductive Biology Unit, Loeb Research Institute, Ottawa Civic Hospital, and Departments of Obstetrics and Gynaecology and Biochemistry, University of Ottawa, and Steacie Institute for Molecular Sciences, National Research Council of Canada, Ottawa, Ontario, Canada

Received March 29, 1994; Revised Manuscript Received August 8, 1994®

ABSTRACT: Sulfogalactosylglycerolipid (SGG) is a sulfoglycolipid found ubiquitously in the plasma membrane of mammalian male germ cells. Although its exact cellular function(s) is unknown, it is speculated that SGG may play a role in cation transport, which may be important in sperm−egg interaction. Given the significant role of Ca^{2+} in many fertilization-related events, the purpose of this study was to determine whether Ca^{2+} interaction with the negatively charged sulfate group of SGG results in changes to the SGG lipid chain molecular dynamics and to compare these lipid dynamics with those resulting from Na^+, Mg^{2+}, or Sr^{2+} interaction with SGG. Pressure-tuning Fourier transform infrared spectroscopy was used in this study. The results obtained showed that all three divalent cations interacted electrostatically with the sulfate moiety of hydrated SGG, although with varying degrees of strength. It was found that the hydrocarbon chains of hydrated SGG-Na^+ multilamellar bilayers were interdigitated, thus increasing disorderedness of the terminal CH_3 group of the hydrocarbon chains. The presence of each of the three divalent cations abolished this interdigitation state. Presumably, this is through the cross-linking interaction of each divalent cation with the sulfate groups of neighboring lipid molecules. Moreover, divalent cation interaction was found to increase the lipid chain dynamics of SGG, with Mg^{2+} inducing the greatest chain disorder followed by Ca^{2+} and then Sr^{2+}. An increase in chain disorder would increase the bilayer fluidity. Such a phenomenon may prove relevant to the changes observed in the sperm plasma membrane during fertilization-related events [Wolf et al. (1986) *J. Cell Biol. 102,* 1372−1377].

Sulfogalactosylglycerolipid (SGG)[1] (Figure 1) is a plasma membrane glycoglycerolipid found only in spermatozoa, testes, and brains of mammals of various species including rats, boars, mice, and humans (Murray et al., 1980, 1990; Farooqui, 1981; Ishizuka & Yamakawa, 1985). SGG constitutes approximately 5−8% of total lipid in testes, whereas in the brain it is only 0.2% of total lipid. SGG is synthesized in primary spermatocytes, being an early marker of male germ cell differentiation. Once synthesized, SGG does not turn over and remains on the surface of live germ cells throughout their development to the spermatozoal stage (Komblatt et al., 1974; Lingwood, 1985). Furthermore, SGG is stable during capacitation, the process that prepares the sperm to bind to the egg (Tanphaichitr et al., 1990). The sulfoglycolipid only turns over when sperm become senescent (Kornblatt et al., 1974; Tanphaichitr et al., 1990).

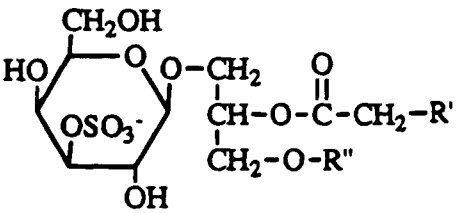

FIGURE 1: Structure of sulfogalactosylglycerolipid (SGG).

It has been shown that Ca^{2+} is present on the sperm surface, although its binding ligands are unknown (Ruknudin, 1989). Given its negatively charged sulfate group (Figure 1), SGG has the potential to "trap" cations such as Ca^{2+} and Mg^{2+} on the sperm plasma membrane. Among numerous divalent cations present in the female reproductive tract fluid, Ca^{2+} appears to be necessary for various activities of mammalian sperm including (1) capacitation, which involves biochemical modification of the sperm plasma membrane in preparation for the acrosome reaction (Fraser, 1987); (2) acquisition of hyperactivated motility patterns of capacitated sperm (Yanagimachi, 1994); (3) sperm acrosome reaction, which results in the release of the hydrolytic enzymes of the acrosome, essential for sperm penetration through the egg investment (Cummins & Yanagimachi, 1986); (4) sperm binding to the zona pellucida, the egg extracellular sulfoglycoprotein matrices (Saling et al., 1978); and (5) sperm−egg fusion (Fraser, 1987; Yanagimachi, 1994). Increased perme-

† This research was supported by the Medical Research Council of Canada, Grant MA-10366 (to N.T.), and the National Research Council of Canada (P.T.T.W.).

* To whom correspondence should be addressed at the Reproductive Biology Unit, Ottawa Civic Hospital, 1053 Carling Ave., Ottawa, Ontario K1Y 4E9, Canada. Fax: (613) 761-5365; Telephone: (613) 761-4081.

‡ Human IVF Labs, Reproductive Biology Unit, Loeb Research Institute, Ottawa Civic Hospital, and Departments of Obstetrics and Gynaecology and Biochemistry, University of Ottawa.

§ Steacie Institute for Molecular Sciences, National Research Council of Canada.

|| Department of Biochemistry, University of Ottawa.

® Abstract published in *Advance ACS Abstracts,* October 15, 1994.

[1] Abbreviations: FAME, fatty acid methyl ester; GLC, gas liquid chromatography; MAGD, monoalkyl glycerol diacetate; SGC, sulfogalactosylceramide; SGG, sulfogalactosylglycerolipid; SGG-Na^+, Na^+ salt of SGG; SGG-Ca^{2+}, Ca^{2+} salt of SGG; SGG-Mg^{2+}, Mg^{2+} salt of SGG; SGG-Sr^{2+}, Sr^{2+} salt of SGG; SLIP1, sulfolipid immobilizing protein 1; TLC, thin-layer chromatography.

0006-2960/94/0433-13250$04.50/0 © 1994 American Chemical Society

ability of the plasma membrane to Ca^{2+} coincides with the increased fluidity that occurs during capacitation (Yanagimachi & Usui, 1974; Rogers & Yanagimachi, 1976; Wolf et al., 1986). Membrane depolarization and the opening of Ca^{2+} channels may initiate the acrosome reaction (Florman & First, 1988; Babcock et al., 1978; Florman et al., 1992). Sperm membrane modification during capacitation, the acrosome reaction, and other fertilization-related events may be partially facilitated by Ca^{2+} interaction with SGG. In addition to Ca^{2+}, other divalent cations have been shown to affect the sperm capacitation and acrosome reaction events. Sr^{2+} was found to effectively replace Ca^{2+}, enhancing both the acrosome reaction and hyperactivated motility in guinea pig spermatozoa and capacitation in human spermatozoa (Yamagimachi & Usui, 1974; Stock & Fraser, 1989; Roldan & Harrison, 1989). In contrast, it has been demonstrated that Mg^{2+} counters the action of Ca^{2+} with respect to capacitation (Yanagimachi & Usui, 1974; Rogers & Yanagimachi, 1976).

It has been speculated that sulfoglycolipids such as SGG and sulfogalactosylceramide (SGC) may be involved in cation transport (Hakomori, 1981; Karlsson et al., 1974). Recently, we have carried out studies on lipid dynamics effects of Ca^{2+} binding to a bilayer suspension of SGC, a sulfoglycolipid that is structurally related to SGG and present in germ cells of some vertebrates as well as epithelial cells of somatic cells. We have demonstrated that Ca^{2+} binds to the sulfate moiety of the polar head region and most likely cross-links neighboring SGC molecules (Tupper et al., 1992). Moreover, the binding of Ca^{2+} to SGC weakens the inter- and intramolecular hydrogen bonding, and the hydrocarbon chains become more disordered, thus resulting in increased fluidity of the lipid multilayers. Although SGC and SGG are similar in their structure and both have a C=O group, a hydrogen acceptor in their interfacial regions, only SGC possesses two hydrogen donors (N—H and O—H) in this region. It is likely, therefore, that SGC is involved in a higher degree of interfacial hydrogen bonding (Tupper et al., 1992). This hydrogen bonding would likely affect the overall dynamics of the lipid bilayers. Therefore, it is important to evaluate the effect of Ca^{2+} binding on membrane fluidity directly with SGG bilayers. Changes in fluidity of discrete lipid domains in the cell plasma membrane may influence specific plasma membrane proteins (Surewicz et al., 1992) and enzyme activities (Gordon & Sauerheber, 1982).

The specific functions of SGG are not known. Our preliminary observations suggest that it may be involved in sperm—egg interaction (Tanphaichitr, unpublished results), although the molecular mechanisms of SGG action in this process are not clear. Like other sulfated glycoconjugates (Holt et al., 1989), SGG has a specific binding protein. The ~68-kDa evolutionarily conserved germ cell membrane protein, termed sulfoglycolipid immobilizing protein (SLIP1), has been shown to bind specifically to SGG *in vitro* (Lingwood, 1985; Law et al., 1988) and to play a role in mouse sperm—egg binding (Tanphaichitr et al., 1992, 1993). In rat sperm, SLIP1 and SGG are colocalized in the plasma membrane of male germ cells throughout spermatogenesis, although some differences in their spatial distribution occur in mature sperm (Lingwood, 1986; Tanphaichitr et al., 1993). It is possible that SGG might influence SLIP1 function and, in turn, sperm function.

In this study, we analyzed the effects of Ca^{2+}, Mg^{2+}, and Sr^{2+} interaction with SGG multilayers on lipid chain dynamics. The technique of pressure-tuning Fourier transform infrared spectroscopy was used. This technique can determine not only whether Mg^{2+}, Ca^{2+}, and Sr^{2+} interact with the negatively charged sulfate group of SGG but also how this interaction affects individual functional groups on the SGG molecule (Auger et al., 1988, 1990; Tupper et al., 1992; Wong, 1984, 1987; Wong et al., 1985, 1988). The present report indicates that the binding of each of these three divalent cations (Mg^{2+}, Ca^{2+}, and Sr^{2+}) to the SGG sulfate group results in an increase in lipid chain dynamics. In contrast, the hydrocarbon chains of SGG-Na^+ assumes an interdigitated state.

MATERIALS AND METHODS

Materials

D_2O (99.9 atom %); SGC; tris(hydroxymethyl)aminomethane hydrochloride (Tris-HCl); $CaCl_2 \cdot 2H_2O$; $MgCl_2 \cdot 6H_2O$; and $SrCl_2 \cdot 6H_2O$ were all reagent grade and purchased from Sigma Chemical Co. (St. Louis, MO). Purified SGG was a gift from Dr. Cliff Lingwood, Hospital for Sick Children, University of Toronto. High-purity natural crystalline α-quartz was obtained from Karl Lambrecht Corp. (Chicago, IL). Silica gel precoated thin-layer chromatography (TLC) K6 plates (250 μm layer, 20 × 20 cm) were purchased from Whatman (Kent, England). Bio-Sil A silica (bead size 150−300 μm) for adsorption column chromatography was obtained from Bio-Rad (Richmond, CA). Fatty acyl methyl ester (FAME) standards were from NuChek (Slysian, MN). Monoalkyl glycerol diacetate (MGD) standards were prepared by acetylation (Kates et al., 1986) of chimyl (16:0), batyl (18:0), and selachyl (18:1) alcohols (Western Chemicals Industries Ltd., Vancouver, BC).

Methods

Lipid Extraction from Testes. Lipids were extracted from the testes using the method of Bligh and Dyer (1959), as modified by Kates (1986). A pair of ram testes (*ca.* 1 Kg) was generously provided by Dr. Paul Fiser, Centre for Food and Animal Research of Canada. Each testis was cut into small pieces and homogenized in *ca.* 1500 mL of MeOH/$CHCl_3$ (2:1 v/v) in a glass Potter homogenizer with a Teflon piston. The homogenate was incubated for 2 h at 4 °C and then suction-filtered on a Buchner funnel. The ratio of MeOH/$CHCl_3$/H_2O in the single phase filtrate was 2:1:0:8 (v/v). Addition of equal volumes of $CHCl_3$ and H_2O to the single phase filtrate to give a final ratio of $CHCl_3$/MeOH/H_2O (1:1:0.9 v/v) resulted in the formation of two phases. The mixture was transferred into a separatory funnel and left overnight at room temperature or 4 °C to allow complete separation of the two phases. The lower $CHCl_3$ phase, containing the lipids, was removed, diluted with benzene (10%), and concentrated on a rotary evaporator.

Purification of SGG. The extracted lipids were fractionated by adsorption column chromatography using Bio-Sil A silica (Kates, 1986). Elution of the lipids was carried out using the organic solvents in the following order: $CHCl_3$, 10 column volumes; $CHCl_3$/acetone (1:1 v/v), 3 column volumes; acetone, 15 column volumes; and MeOH, 10 column volumes. Lipid contents of each fraction were

monitored by ascending TLC using the solvent system of $CHCl_3$/MeOH/H_2O, 65:25:4 (v/v) (Levine et al., 1976). The thin-layer chromatogram was air dried, and glycolipid spots including standard SGG and SGC were detected by staining with a mixture of α-naphthol and 50% H_2SO_4, followed by heating at 150 °C to detect all lipid spots (Kates, 1986). Acetone fractions containing SGG were pooled, rotoevaporated to dryness, redissolved in a minimal amount of chloroform, and finally precipitated from chloroform with 10 vol of acetone (Kates, 1986). Purity of SGG obtained (natural salt form) was verified by TLC using the solvent system of $CHCl_3$/MeOH/H_2O/concentrated ammonia (65:25:3:1 v/v) (Kornblatt, 1979) and by IR spectroscopic analysis.

The acyl and alkyl moieties of SGG were characterized by the previously described method (Kates, 1986; Vishnubhatla et al., 1988). Briefly, SGG was subjected to methanolysis followed by acetylation. Fatty acid methyl ester and monoalkyl glycerol diacetate, generated from the acyl and alkyl moieties of SGG, respectively, were analyzed for the proportion of their subclasses by gas liquid chromatography (GLC) using a PYE Unicam instrument.

Removal of Endogenous Cations from SGG and Preparation of SGG-Na$^+$. A solution of the natural salt form of SGG was converted to the free acid form and then to the sodium salt form (SGG-Na$^+$) as previously described (Kates, 1986).

High-Pressure Infrared Spectroscopy Studies. (a) Sample Preparation. Approximately 1 mg of SGG-Na$^+$ was hydrated (50% by wt) in 50 mM Tris-HCl in D_2O/H_2O, pH 7.05, to form lipid multilamellar bilayers. Multilayers of SGG were also generated by mixing together equal volumes of the SGG-Na$^+$ solution (0.6 M) and 2.0 M $CaCl_2$, $SrCl_2$, or $MgCl_2$ solution made in Tris-HCl in D_2O, pH 7.05. This resulted in 0.3:1.0 molar ratio of SGG-Na$^+$ to Ca^{2+}, Mg^{2+}, or Sr^{2+}. These three SGG-divalent complexes were named SGG-Ca^{2+}, SGG-Mg^{2+}, and SGG-Sr^{2+}, respectively. Complete dispersion was ensured by heating and vortexing the lipid multilayers 3−4 times. Solid samples of SGG-Na$^+$, SGG-Ca^{2+}, SGG-Mg^{2+}, and SGG-Sr^{2+} were prepared by lyophilizing the aqueous dispersion of the lipid multilayers for *ca.* 24 h, followed by purging the samples with a N_2 stream for *ca.* 72 h.

(b) Spectroscopic Analysis. For spectroscopic analysis, individual solid or hydrated samples (~0.01 mg) were mixed with powdered α-quartz (an internal pressure calibrant) and placed in a well (0.37 mm diameter) of a stainless steel gasket (0.23 mm thickness), which was then mounted on a diamond anvil cell at room temperature (Wong et al., 1985). A Digilab FTS-60 Fourier transform spectrophotometer was used to measure the infrared spectra at 28 °C using a mercury cadmium telluride detector cooled by liquid N_2. The infrared beam was condensed on the diamond anvil cell by a sodium chloride lens system.

Infrared spectra of hydrated and anhydrous solid samples of SGG-Na$^+$, SGG-Ca^{2+}, SGG-Mg^{2+}, and SGG-Sr^{2+} were measured as a function of pressure up to 17 kbar. For each spectrum, 512 interferograms were co-added at a spectral resolution of 4 cm^{-1}. The 695-cm^{-1} photon band of the α-quartz was used to determine the hydrostatic pressure in the gasket of the diamond anvil (Wong et al., 1985). Fourier derivation and deconvolution techniques were applied in order to separate unresolvable infrared band contours. Spectral features originating from the vibrational modes of the sulfate group, the carboxyl group, and the hydrocarbon chains were examined, and height intensity ratios were calculated from the vibrational modes originating from the hydrocarbon chains.

RESULTS AND DISCUSSION

Purity of SGG. Purity of our extracted ram testis SGG was verified by TLC using the solvent system of $CHCl_3$/MeOH/H_2O/concentrated ammonia (65:35:3:1 v/v). The chromatographed lipid gave a single band with an R_f of 0.43, which is identical to that described previously by Gadella et al. (1992). In addition, the IR spectrum of our SGG-Na$^+$ (results not shown) was identical to that of boar testis SGG described previously by Ishizuka et al. (1973). More than 95% of the acyl group of SGG was 16:0, the remainder being 18:0, 14:0, and 14:1. The alkyl group was comprised of mostly 16:0 (66%), the remainder including 14:0 (7%), 15:0 (2%), 15:1 (7%), 17:0 (1%), three unidentified components (10%), and minor short-chain subclasses (3%). Interestingly, SGG isolated from other mammalian testes also possesses C16:0 as its acyl and alkyl moieties (Ishizuka et al., 1973; Suzuki et al., 1973; Alvarez et al., 1990).

Divalent Cation Interaction. The spectra of SGG-Na$^+$, SGG-Ca^{2+}, SGG-Mg^{2+}, and SGG-Sr^{2+} were compared to confirm cation interaction with SGG and to determine the effects of this interaction on hydrocarbon chain dynamics. Two SO_3^- absorption modes proved useful for this study, namely, the asymmetric O—S—O$^-$ stretching mode at 1200−1240 cm^{-1} and the C—O stretching mode at 920−1040 cm^{-1} of the ester-linked SO_3^- group. The O—S—O$^-$ symmetric mode, which ranges from 1040 to 1080 cm^{-1} (Bellamy, 1975; Kates, 1986), was not used for the analysis since it overlaps with many C—OH stretching bands from the sugar head group. Also, the S—O stretching mode, which ranges from 790 to 830 cm^{-1} (Kates, 1986), was not used due to interfering quartz bands.

Due to interfering D_2O bands to the asymmetric O=S—O$^-$ stretching mode, H_2O samples were used for the cation interaction studies. Figure 2B presents the deconvolved infrared spectra of SGG-Na$^+$, SGG-Ca^{2+}, SGG-Mg^{2+}, and SGG-Sr^{2+} in the asymmetric O—S—O$^-$ stretching region at ambient pressure. The deconvolved spectra were obtained to reveal the underlying components of a broad band that appeared in the original spectra (Figure 2A). Spectra of all four samples were comprised of two components, a high-frequency band (1223 cm^{-1}), and a low-frequency band (1209 cm^{-1}), representing the free SGG and the SGG−cation population, respectively. The identity of these two bands was derived from an observation that the intensity of the 1209-cm^{-1} band was increased along with a decrease in intensity of the 1223-cm^{-1} band when an increasing amount of Na$^+$ was added to the free acid form of the SGG solution. The results imply that a portion of the SGG sample in the bilayer phase was bound with a cation. Given their divalent nature, Ca^{2+}, Mg^{2+}, and Sr^{2+} most likely cross-linked the SO_3^- groups of neighboring SGG molecules. Comparison of their absorption intensity showed that SGG-Ca^{2+} absorbed with the highest intensity. SGG-Mg^{2+} absorbed at a slightly lower intensity than SGG-Ca^{2+}. SGG-Sr^{2+} absorbed at a much lower intensity than SGG-Ca^{2+} and SGG-Mg^{2+} even lower than SGG-Na$^+$. This difference in absorption intensity demonstrates that Ca^{2+} and Mg^{2+} had a stronger ionic interaction with the SO_3^- group than Na$^+$ and Sr^{2+}. A

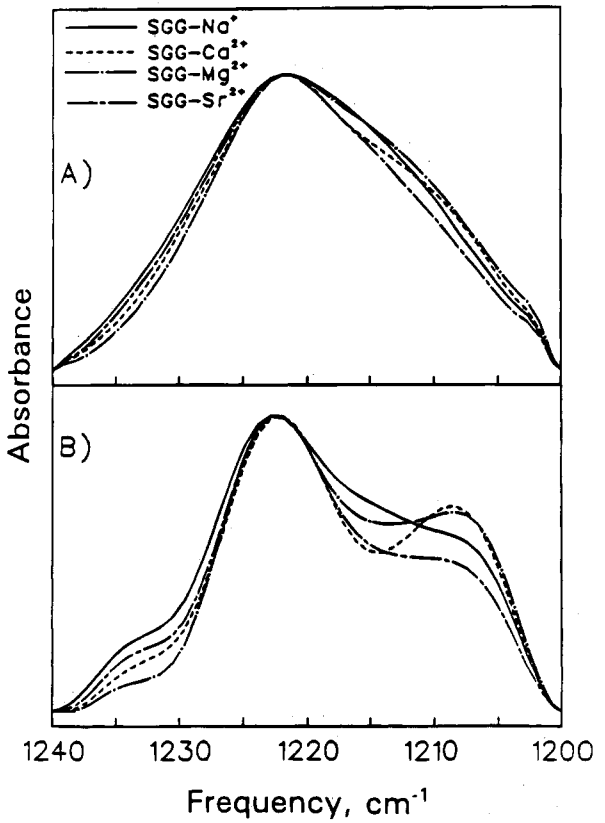

FIGURE 2: (A) Infrared spectra of hydrated SGG-Na^+, SGG-Ca^{2+}, SGG-MG^{2+}, and SGG-Sr^{2+} in the S=O asymmetric stretching region (1200−1240 cm^{-1}) at ambient pressure. (B) The Fourier deconvolved spectra of hydrated SGG-Na^+, SGG-Ca^{2+}, SGG-Mg^{2+}, and SGG-Sr^{2+} in the S=O asymmetric stretching region at ambient pressure.

stronger ionic interaction results in a larger transition moment and thus a stronger bond intensity. The lowest absorption intensity of SGG-Sr^{2+} may be due to the large size of Sr^{2+}, thus causing steric hindrance to its interaction with the SO_3^- groups of the two adjacent SGG molecules.

In the spectra of all four samples, an intense band appeared at 990 cm^{-1}, corresponding to the C−O stretching mode of the C−O group linked to the SO_3^- (data not shown). Upon addition of the divalent cations, the bandwidth increased slightly, indicating that the overall conformation of the sulfate moiety became slightly more disordered.

Ester Group. The acyl ester group of SGG is present in the interfacial region of the lipid molecule and is likely involved in intermolecular and/or intramolecular hydrogen bonding with OH groups of galactose. Consequently, the carbonyl group likely has a significant effect on the SGG conformational structure and the interactions with neighboring molecules. Figure 3 presents the infrared spectra of SGG-Na^+, SGG-Ca^{2+}, SGG-Mg^{2+}, and SGG-Sr^{2+} in the C=O stretching mode region ranging from 1650 to 1780 cm^{-1} (Kates, 1986) at ambient pressure. All four spectra were comprised of two components, a high-frequency component (1735 cm^{-1}) and a low-frequency component (1715 cm^{-1}). The low-frequency component corresponds to a strongly hydrogen bonded C=O group (Wong & Mantsch, 1988). Comparison of the spectra of all four samples revealed different values for the intensity of the low-frequency component. This indicates that the divalent cation interaction with the SO_3^- group of the lipid molecule affected the hydrogen bonding of the ester group differently, depending upon the cation. Of all the SGG−cation complexes, the low-frequency component of SGG-Na^+ (1715 cm^{-1}) absorbed with the highest intensity, indicating that the greatest proportion of the C=O groups in the sample was hydrogen bonded (Figure 3). The SGG-Mg^{2+} spectrum had a slightly lower intensity of absorption at this low-frequency component (1715 cm^{-1}) as compared to the intensity of SGG-Na^+, indicating a small decrease of the hydrogen-bonded C=O group population of SGG-Mg^{2+}. In contrast to SGG-Na^+ and SGG-Mg^{2+}, SGG-Sr^{2+} absorbed at a much lower intensity at this low-frequency band, followed by SGG-Ca^{2+}. This indicates that a smaller proportion of the C=O group of SGG-Sr^{2+} and SGG-Ca^{2+} was participating in hydrogen bonding.

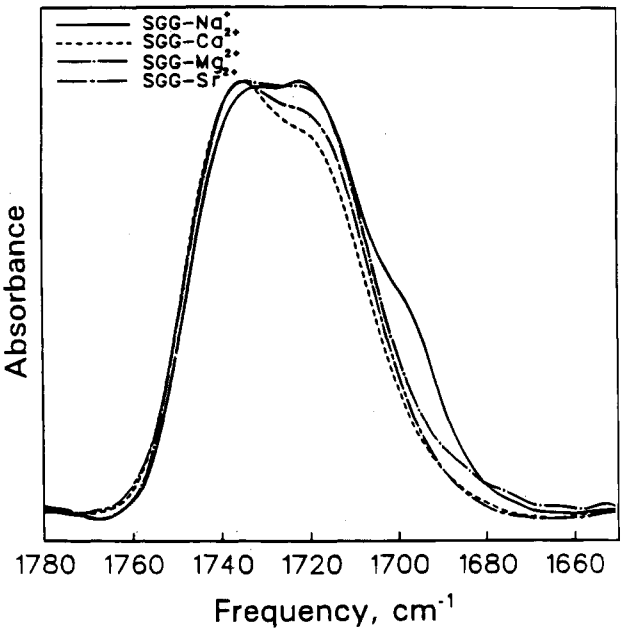

FIGURE 3: Infrared spectra of hydrated SGG-Na^+, SGG-Ca^{2+}, SGG-Mg^{2+}, and SGG-Sr^{2+} in the ester C=O stretching region (1650−1780 cm^{-1}) at ambient pressure.

Hydrocarbon Chain Structure. The interaction of the divalent cations with the SO_3^- group would affect not only the hydrogen bonding in the interfacial region but also the dynamics of the hydrocarbon chains. The fluidity of the multilayer is determined by the conformational and orientational order/disorder of the hydrocarbon chains. Analysis of the lipid chain dynamics due to divalent cation interaction with SGG multilayers may help us understand any fluidity effects these divalent cations may have on SGG-rich domains in the sperm membrane.

At room temperature, SGG is likely in the gel phase (Parks & Lynch, 1992) with its hydrocarbon chains (largely 16:0) fully extended. However, due to reorientational fluctuations and twisting and torsion motions, the chains would be in a disordered orientation. Application of pressure to the lipid multilayers reduces the mobility of the hydrocarbon chains, resulting in decreases in magnitude of the intermolecular reorientational fluctuations and twisting and torsion motions and, hence, in a higher degree of order (Wong, 1984). As the orientation of each hydrocarbon chain becomes more ordered and provided that the plane of each hydrocarbon chain becomes nearly perpendicular to its neighboring chain (i.e., nonequivalent), this phenomenon spectroscopically results in a correlation field splitting in the vibrational modes

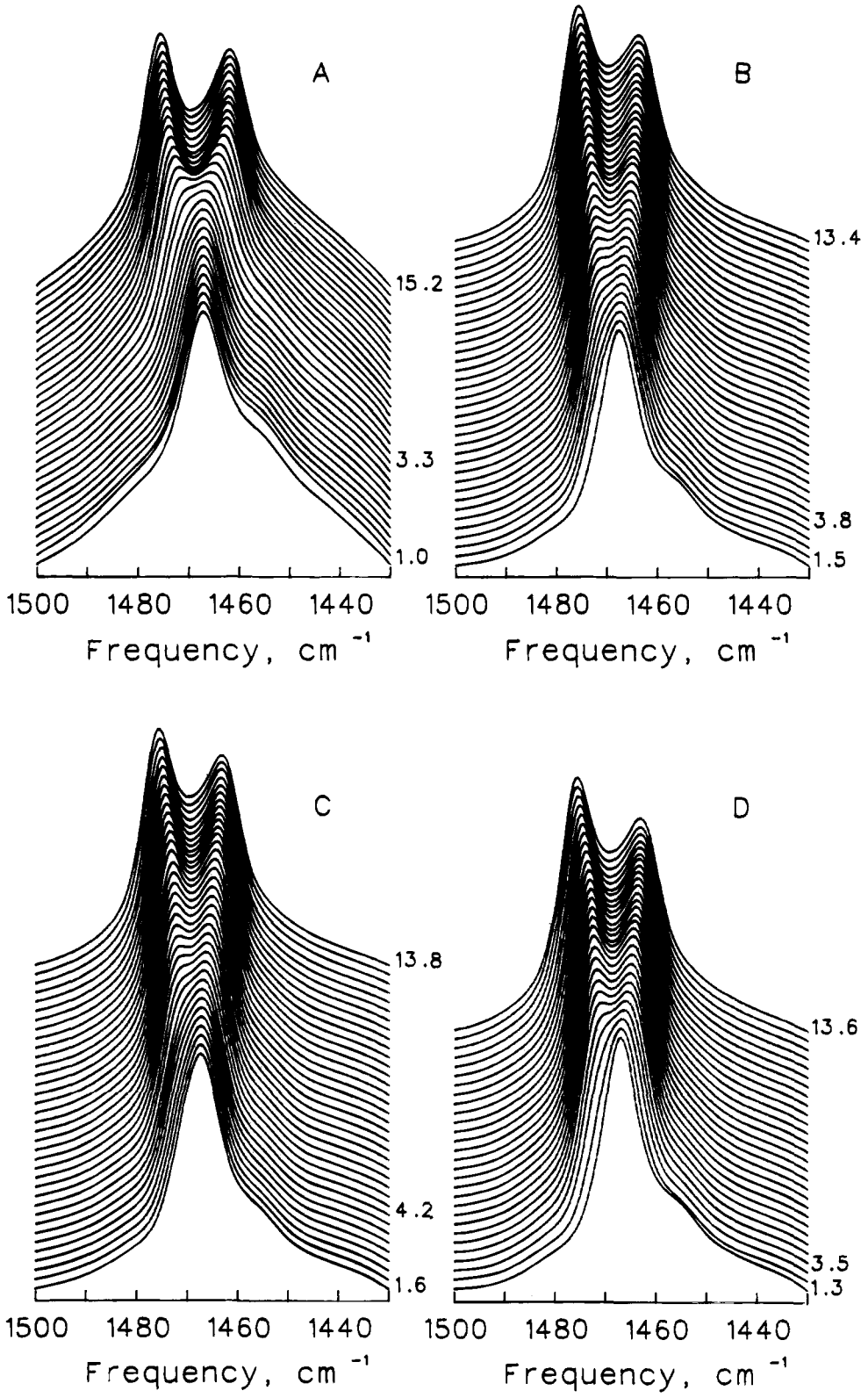

FIGURE 4: Stacked contour plots of the infrared spectra of the δCH_2 scissoring mode (1430−1500 cm^{-1}) of (A) hydrated SGG-Na^+, (B) hydrated SGG-Ca^{2+}, (C) hydrated SGG-Mg^{2+}, and (D) hydrated SGG-Sr^{2+}. The numbers on the right of the plots are pressure values in kbar.

of the hydrocarbon chains (Auger et al., 1988, 1990). Therefore, when the baratropic behavior of the vibrational modes of the hydrocarbon chains is monitored, the pressure at which the correlation field splitting occurs can be determined. The amount of pressure required to induce this splitting can be used as a measure of how ordered or disordered the orientations of the hydrocarbon chains are; greater chain disorder requires more pressure to compress the chains into an ordered state. The CH_2 scissoring mode (δ) absorbs in the region of 1450−1490 cm^{-1} and is sensitive to changes in conformation and orientational disorder of the hydrocarbon chains (Stein & Sutherland, 1953, 1954). Figure 4 presents the stacked contour plots of the infrared spectra of (A) hydrated SGG-Na^+, (B) hydrated SGG-Ca^{2+},

(C) hydrated SGG-Mg^{2+}, and (D) hydrated SGG-Sr^{2+}. At ambient and low pressure, a narrow and intense absorption band at 1467 cm^{-1} was present in all four plots and was attributed to the CH_2 scissoring mode of the fully extended hydrocarbon chains of SGG. As the pressure increased, a correlation field splitting of the absorption mode became apparent in all four samples. Comparison of the stacked contour plots of the δCH_2 scissoring mode of SGG-Na^+, SGG-Ca^{2+}, SGG-Mg^{2+}, and SGG-Sr^{2+} (Figure 4, A–D, respectively) revealed that SGG-Na^+ spectra differed in their baratropic behavior in that the correlation field splitting of SGG-Na^+ took place more suddenly and rapidly at higher pressures (>11 kbar). This resulted in a pronounced "valley" appearing between the two bands. In contrast, the correlation field splitting band of the higher frequency ($\delta'CH_2$) in the spectra of SGG-Ca^{2+}, SGG-Mg^{2+}, and SGG-Sr^{2+} initially appeared at lower pressures as only a broad shoulder on the high-frequency side of the lower frequency component (δCH_2) of correlation field splitting. The high-frequency component ($\delta'CH_2$) gradually gained intensity until a correlation field splitting became evident. The pronounced valley defined by the two component bands of the SGG-Na^+ δCH_2 scissoring mode suggested interdigitation of the SGG-Na^+ bilayer (Siminovitch et al., 1987). The qualitative features of band shapes, when displayed in a stacked contour plot, can be used to distinguish interdigitated bilayer systems. In fully interdigitated lipid bilayers, the interchain interactions are significantly enhanced and are reflected in the CH_2 scissoring and rocking modes. The broad valley, resulting from the large magnitude of splitting produced by the correlation field splitting of the SGG-Na^+ δCH_2 scissoring mode, signified a more rapid enhancement of interchain interactions expected on compression of an interdigitated bilayer (Siminovitch et al., 1987). The presence of only a single narrow δCH_2 scissoring band at 1467 cm^{-1} at ambient pressure for all four lipid samples indicated that the chains were fully extended, regardless of whether the SGG hydrocarbon chains were interdigitated or not, and that there were still significant chain reorientational fluctuations at ambient pressure. However, under increasing pressure, these fluctuations are dampened, and the differences in interchain packing (including an interdigitated and noninterdigitated state) and dynamic structure of the lipid acyl chains can be differentiated by their infrared band shapes.

The presence of interdigitation of lipid hydrocarbon chains was also demonstrated by a quantitative approach (Siminovitch et al., 1987). Figure 5 displays the pressure dependence of the peak intensity ratio (R) of the $\delta'CH_2$ and δCH_2 components of the correlation field splitting of the CH_2 scissoring mode, i.e., $R = I_{\delta'}/I_{\delta}$. Analysis of this figure revealed both large- and small-scale fluctuations in the R parameter with increasing pressure. The small-scale fluctuations (±0.02) were inherent in the calculations and were due to errors in the height measurements. Up to 7.5 kbar of pressure, rapid increases in the R parameter (>0.02 kbar) were evident for SGG-Mg^{2+}, SGG-Ca^{2+}, and SGG-Sr^{2+}, followed by plateaus from 7.5 to 10 kbar. Large increases in the R parameter of SGG-Mg^{2+}, SGG-Ca^{2+}, and SGG-Sr^{2+} occurred again at pressures higher than 10 kbar. These large-scale increases were most likely due to pressure-induced changes in hydrocarbon chain packing (Siminovitch et al., 1987; Wong & Mantsch, 1985, 1984). The difference in the magnitude of R among SGG-Mg^{2+}, SGG-Ca^{2+}, and SGG-Sr^{2+} suggests subtle differences in interchain interactions and chain dynamics. In contrast to two-phased increases of the R parameter of SGG-Mg^{2+}, SGG-Ca^{2+}, and SGG-Sr^{2+}, the R parameter of SGG-Na^+ remained the same up to 11 kbar of pressure, where an increase was observed (Figure 5). However, the peak height ratios ($R = I_{\delta'}/I_{\delta}$) of SGG-$Ca^{2+}$, SGG-$Mg^{2+}$, and SGG-$Sr^{2+}$ were significantly higher than the R value of SGG-Na^+ at all pressure values. Based on the previous finding of Siminovitch et al. (1987) that the peak height ratio ($R = I_{\delta'}/I_{\delta}$) of noninterdigitated 1,2-dipalmitoyl-*sn*-glycero-3-phosphocholine is always higher than that of the interdigitated state of the lipid, the results in Figure 5 strongly suggest that the hydrocarbon chains of SGG-Na^+ were interdigitated.

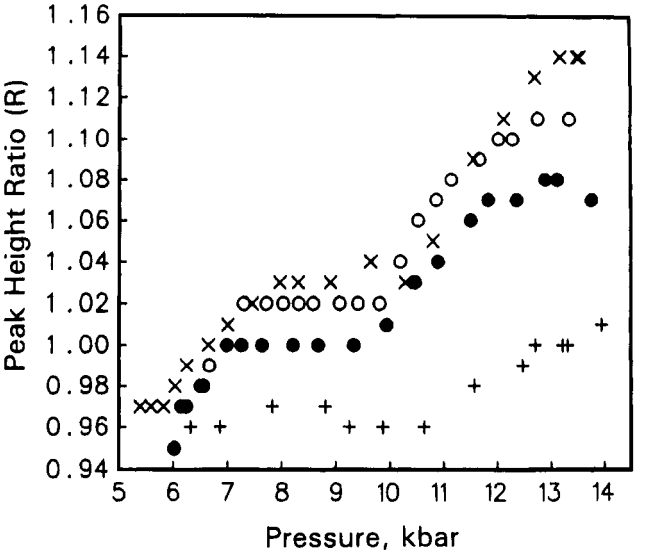

FIGURE 5: Pressure dependence of the peak height intensity ratio of the δCH_2 scissoring mode, $R(I_{\delta'}/I_{\delta})$ for (+) hydrated SGG-Na^+, (○) hydrated SGG-Ca^{2+}, (●) hydrated SGG-Mg^{2+}, and (×) hydrated SGG-Sr^{2+}.

Siminovitch et al. (1987) have also demonstrated that the relative intensities of the CH_2 rocking correlation field splitting components are sensitive to interdigitation of the hydrocarbon chains. However, they found that the γCH_2 rocking mode intensities were difficult to quantitate because of the shoulders of the intense quartz 801- and 695-cm^{-1} bands and the variable baseline. In the present study, we have introduced a new parameter, R', which is the ratio of the intensity of the high-frequency correlation field splitting pressure ($I_{\gamma'}$) to the intensity of the valley lowest point (I_{valley}). This new quantitative approach is reliable and relatively simple.

Comparison of the stacked contour plots of the γCH_2 rocking mode revealed a different baratropic behavior of the SGG-Na^+ spectra relative to those of SGG-Ca^{2+}, SGG-Mg^{2+}, and SGG-Sr^{2+}. The intensity of the SGG-Na^+ $\gamma'CH_2$ rocking band (740 cm^{-1}) increased more rapidly at high pressures, producing a deep and wide valley between the two component bands (data not shown). Due to the interfering shoulder of the 695-cm^{-1} quartz band, the intensity of the γCH_2 rocking (720 cm^{-1}) band could not be reliably quantitated. As discussed above, we have used the parameter $R' = I_{\gamma'}/I_{valley}$ instead to demonstrate an interdigitated state of the lipid hydrocarbon chains. Although R' does not include the intensity of the low frequency of correlation field splitting pressure (I_{γ}), the intensity of the valley lowest point (I_{valley})

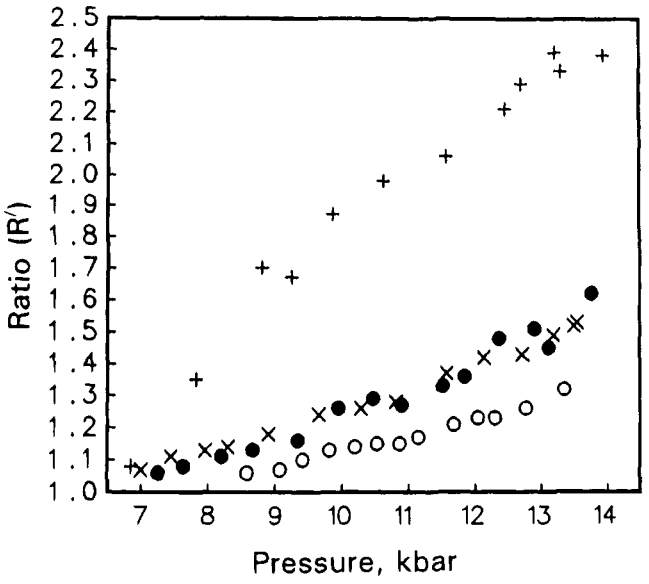

FIGURE 6: Pressure dependence of the height intensity ratio of the γCH_2 rocking mode, $R'(I_\gamma/I_{valley})$ for (+) hydrated SGG-Na^+, (○) hydrated SGG-Ca^{2+}, (●) hydrated SGG-Mg^{2+}, and (×) hydrated SGG-Sr^{2+}.

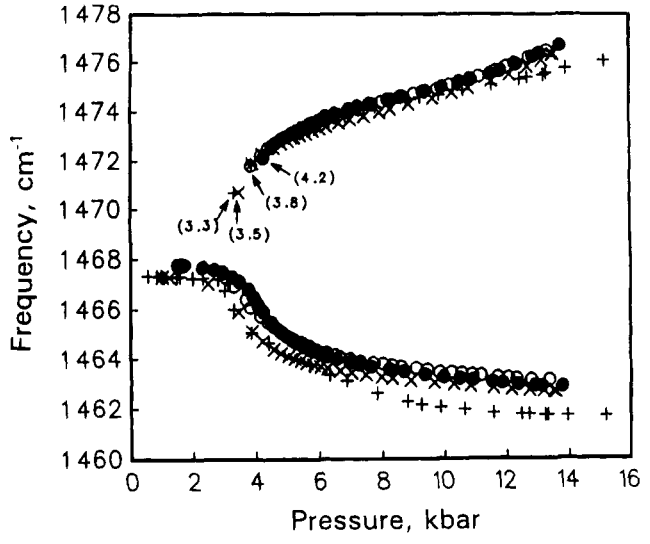

FIGURE 7: Pressure dependence of the frequencies of the δCH_2 scissoring mode (1460−1478 cm^{-1}) for (+) hydrated SGG-Na^+, (○) hydrated SGG-Ca^{2+}, (●) hydrated SGG-Mg^{2+}, and (×) hydrated SGG-Sr^{2+}.

is already a function of the two component heights of the correlation field splitting as well as the magnitude of their splitting. Consequently, I_{valley} would be sensitive to the interchain interactions and thus the height ratio, $R' = I_\gamma/I_{valley}$, would be a useful parameter to determine interdigitation. Indeed, the pressure dependence profile of the SGG-Na^+ R' parameter was significantly different from that of SGG-Ca^{2+}, SGG-Mg^{2+}, and SGG-Sr^{2+} (Figure 6). The rapid increase in the SGG-Na^+ R' parameter was reflected by the resulting deep valley between the two component bands. The extent of the correlation field splitting of the γCH_2 rocking mode is interchain in origin, and the results suggest that SGG hydrocarbon chains assumed an interdigitated lamellar structure (Siminovitch et al., 1987). The deep valley appearance of the CH_2 rocking correlation field splitting was similarly observed in the interdigitated state of the 1,2-dihexadecyl-*sn*-glycero-3-phosphocholine lipid bilayers (Siminovitch et al., 1987). In contrast, upon addition of the divalent cations Ca^{2+}, Mg^{2+}, and Sr^{2+} to SGG, a rapid increase of R' was not observed, suggesting that the bilayers of SGG-Ca^{2+}, SGG-Mg^{2+}, or SGG-Sr^{2+} were not interdigitated (Figure 6). It is likely that the divalent cations cross-linked the SGG head groups and prevented interdigitation of the SGG lipid molecules.

The effect of the divalent cations on the hydrocarbon chain dynamics was determined by comparing the pressure dependence of the δCH_2 scissoring mode frequencies of SGG-Na^+, SGG-Ca^{2+}, SGG-Mg^{2+}, and SGG-Sr^{2+} (Figure 7). It was noted that at pressures above 8 kbar, SGG-Na^+ exhibited a higher magnitude of correlation field splitting than SGG-Mg^{2+}, SGG-Ca^{2+}, and SGG-Sr^{2+}. In other words, the frequency difference between the high- and low-frequency components of the splitting for SGG-Na^+ was greater than that of all other samples. This is typical of an interdigitated state of lipid hydrocarbon chains (Siminovitch et al., 1987), thus confirming the results described above. The higher splitting pressure of SGG-Mg^{2+} (4.2 kbar) indicated that it induced the greatest chain disorder followed by SGG-Ca^{2+} (3.8 kbar). The lower splitting pressure of SGG-Sr^{2+} (3.5 kbar) reflected only a small increase in chain disorder compared to SGG-Na^+ (3.3 kbar). Therefore, not only did all three divalent cations eliminate bilayer interdigitation, but all three divalent cations induced greater hydrocarbon chain disorder than the monovalent cation Na^+. As observed in our previous study (Tupper et al., 1992), Ca^{2+} binding to SGC multilayers results in a significant increase in the hydrocarbon chain disorder. In contrast, Ca^{2+} induces a smaller increase in the correlation field splitting pressure of SGG. This may be due to the fact that SGG-Na^+ hydrocarbon chains are interdigitated (results from the present study), while SGC-Na^+ hydrocarbon chains are not (Tupper et al., 1992). Lack of interdigitation of SGC-Na^+ bilayers may be due to the extensive hydrogen bonding in the interfacial region of SGC. On the other hand, the presence of a "kink" (double bond) in one of the SGC hydrocarbon chains may contribute to greater Ca^{2+} induction of SGC hydrocarbon chain fluidity than that observed in SGG.

Finally, the CH_3 bending mode of SGG was analyzed to characterize the differences between the interdigitated and noninterdigitated systems (Figure 8). Clearly, the interactions of the terminal methyl groups of the interdigitated SGG-Na^+ would be expected to differ from those of the noninterdigitated SGG bilayer. The lower peak frequency of SGG-Na^+ suggested that the methyl group interactions are relatively weak compared to SGG-Ca^{2+} and SGG-Mg^{2+}. The results suggest that the methyl groups of SGG-Na^+ were more disordered. This was not unexpected since the area per head group of interdigitated SGG-Na^+ would likely be increased (Siminovitch et al., 1987), allowing the methyl groups to be more disordered. Interestingly, the peak frequencies of SGG-Sr^{2+} were found to be intermediate between SGG-Na^+ and SGG-Ca^{2+}/SGG-Mg^{2+}. This difference in peak frequency also indicated that the terminal methyl group interaction in SGG-Sr^{2+} was quite different from that in SGG-Mg^{2+} or SGG-Ca^{2+}. The results suggested that the interchain packing of SGG-Sr^{2+} differed from that of SGG-Ca^{2+} and SGG-Mg^{2+}, although the precise nature of the interchain packing in SGG when interacting with various types of divalent cations can only be determined by X-ray diffraction studies.

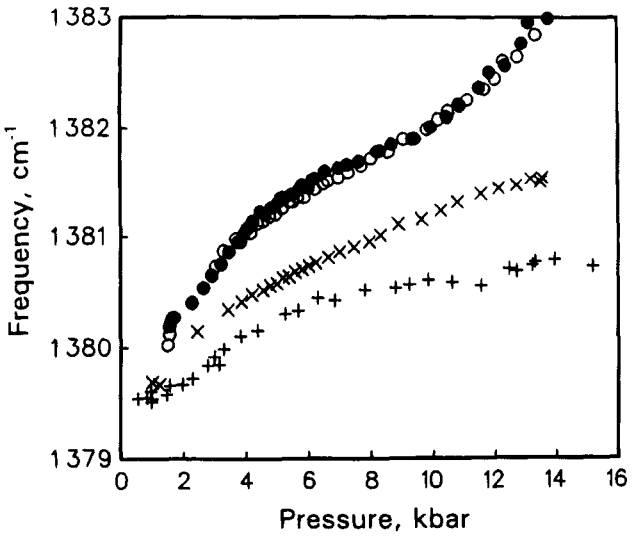

FIGURE 8: Pressure dependence of the frequencies of the CH_3 bending mode (1379−1383 cm^{-1}) for (+) hydrated SGG-Na^+, (○) hydrated SGG-Ca^{2+}, (●) hydrated SGG-Mg^{2+}, and (×) hydrated SGG-Sr^{2+}.

The results of the present study reveal the significant finding that SGG-Na^+ hydrocarbon chains assume an interdigitated state. This conclusion was derived from the following observations. First, the pressure profiles of the CH_2 scissoring (Figure 4) and rocking modes (data not shown) showed the valley patterns typical of other interdigitated bilayers. On the other hand, the profiles of SGG−divalent cation complexes did not show this pattern. Consequently, the peak height ratios of the correlation field splitting of these two modes of SGG-Na^+ hydrocarbon chains were different from those of the hydrocarbon chains of the SGG−divalent cation complexes (Figures 5 and 6). In addition, the width of the correlation field splitting of SGG-Na^+ hydrocarbon chains was larger than that of the hydrocarbon chains of the SGG−divalent cation complexes (Figure 4). Finally, analysis of the CH_3 bending mode indicates weaker interaction between the terminal methyl groups of the hydrocarbon chains of SGG-Na^+ as compared to those of SGG−divalent complexes (Figure 8). These characteristics of the SGG-Na^+ hydrocarbon chains are consistent with those of the interdigitated hydrocarbon chains of 1,2-di-*O*-hexadecyl-*sn*-glycero-3-phosphocholine and 1,3-dipalmityol-*sn*-glycero-2-phophocholine (Siminovitch et al., 1987). The interdigitation observed in the SGG-Na^+ hydrocarbon chains may be partially attributed to the presence of an ether linkage in the *sn*-1 position of the SGG glycerol backbone (Siminovitch et al., 1987; Wong & Mantsch, 1988). The ether bond is not as bulky as the ester linkage present in most phospholipids, and this will allow interdigitation of individual hydrocarbon chains of the opposing leaflets. In addition, both alkyl and acyl groups of SGG are mainly saturated, consisting mainly of C16:O (our results described above; Kornblatt et al., 1974). The extended nature of these saturated hydrocarbon chains will also promote their interdigitation. In contrast, divalent cations interacting ionically with SGG abolished the interdigitated state of SGG-Na^+. Presumably, a divalent cation cross-linked the sulfate groups of the two adjacent SGG molecules or neighboring SGG molecules across two bilayers, thus restricting the movement and space between the hydrocarbon chains of each SGG molecule. This would obstruct interdigitation of individual hydrocarbon chains of the opposing leaflets. The absence of interdigitation in the presence of the divalent cations would reduce the area per head group of each lipid bilayer leaflet, thus decreasing disorderedness of the terminal CH_3 groups. In addition, in the absence of interdigitation, the two lipid bilayer leaflets would no longer be interlocked, and the rate of rotational and torsional movements of the hydrocarbon chains of each leaflet would be enhanced. As a result, a higher pressure was required to reduce these movements as was observed spectroscopically by the higher values of the correlation field splitting pressure of SGG-Mg^{2+}, SGG-Ca^{2+}, and SGG-Sr^{2+} as compared to that of SGG-Na^+ (Figure 7). This increase in the lipid dynamics as well as the steric hindrance caused by cross-linking of the two adjacent SGG molecules by a divalent cation would be responsible for the observed decrease in interfacial hydrogen bonding between the C=O group and the CH_2−OH groups of sugar and/or H−O−H (Figure 3). The larger divalent cations, i.e., Ca^{2+} and Sr^{2+}, had a more pronounced effect in decreasing this hydrogen bonding than Mg^{2+}, implying that steric hindrance may be an important factor in impeding the interfacial hydrogen bonding.

Differences in the effects of divalent cations on the SGG lipid structure and dynamics were observed in this study. These three divalent cations (Ca^{2+}, Mg^{2+}, and Sr^{2+}) differ in a number of parameters including charge distribution, solvation, and electronegativity. In general, the smaller the ion, the higher its degree of charge distribution, solvation, and electronegativity. Mg^{2+} is the smallest among the three divalent cations, followed by Ca^{2+} and Sr^{2+}. The difference in the increased fluidity of the SGG hydrocarbon chains, induced by Mg^{2+}, Ca^{2+}, and Sr^{2+}, appears to be directly proportional to their electronegativity and inversely proportional to their ion size. In contrast, other observed differences cannot be explained only on the basis of the properties of the divalent cations. Rather, the differences may reflect a combination of their properties as well as the exact three-dimensional molecular structure of SGG itself. Nonetheless, these studies may contribute to an understanding as to why these cations have different physiological effects (Stock & Fraser, 1989; Yanagimachi & Usui, 1974; Rogers & Yanagimachi, 1976; Roldan & Harrison, 1989).

Changes in lipid dynamics of SGG induced by its interaction with divalent cations, observed in this study, may not be the sole factor responsible for the changes in sperm membranes during fertilization. However, the approaches used in the present study may serve as a basis for future work with model membranes that are more physiologically representative of the sperm plasma membrane (i.e., containing SGG and/or SGC plus phospholipids and other lipids) with the isolated sperm plasma membrane or with intact sperm. Particular attention should be given to the function of the sulfoglycolipids on the sperm plasma membrane as well as their interaction with other macromolecules such as SLIP1 or the egg zona pellucida.

REFERENCES

Alvarez, J. G., Storey, B. T., Hemling, M. L., & Grob, R. L. (1990) *J. Lipid Res. 31*, 1073−1081.

Auger, M., Jarrell, H. C., Smith, I. C. P., Siminovitch, D. J., Mantsch, H. H., & Wong, P. T. T. (1988) *Biochemistry, 27*, 6086−6093.

Auger, M., Smith, I. C. P., Mantsch, H. H., & Wong, P. T. T. (1990) *Biochemistry, 29*, 2008−2015.
Babcock, D. F., Stamerjohn, D. M., & Hutchinson, T. (1978) *J. Exp. Zool. 204*, 391−399.
Bellamy, L. J. (1975) in *The Infrared Spectra of Complex Molecules, Vol. 1*, 3rd ed., Chapman & Hall, New York.
Bligh, E. G., & Dyer, W. J. (1959) *Can. J. Biochem. Physiol. 31*, 911−917.
Cummins, J. M., & Yanagimachi, R. (1986) *Gamete Res. 15*, 187−212.
Farooqui, A. A. (1981) *Adv. Lipid Res. 18*, 159−202.
Florman, H. M., & First, N. L. (1988) *Dev. Biol. 128*, 453−463.
Florman, H. M., Corron, M. E., Kim, T. D.-H., & Babcock, D. F. (1992) *Dev. Biol. 152*, 304−314.
Fraser, L. R. (1987) in *The Role of Calcium in Biological Systems, Vol. IV* (Anghileri, L. J., Ed.) pp 163−190, CRC Press Inc., Boca Raton.
Gadella, B. M., Colenbrander, B., van Golde, L. M. G., & Lopes-Cardozo, M. (1992) *Biochim. Biophys. Acta 1128*, 155−162.
Gordon, L. M., & Sauerheber, R. D. (1982) in *The Role of Calcium in Biological Systems, Vol. II* (Anghileri, L. J., & Tuffet-Anghileri, A. M., Eds.) pp 4−16, CRC Press Inc., Boca Raton.
Hakomori, S. (1981) *Annu. Rev. Biochem. 50*, 733−764.
Holt, G. D., Krivan, H. C., Gasic, G. J., & Ginsburg, V. (1989) *J. Biol. Chem. 264*, 12138−12140.
Ishizuka, I., & Yamakawa, T. (1985) in *Glycolipids* (Weigandt, H., & Deenen, L. L. M., Eds.) pp 101−197, Elsevier, New York.
Ishizuka, I., Suzuki, M., & Yamakawa, T. (1973) *J. Biochem. 73*, 77−87.
Karlsson, K.-A., Samuelsson, B. E., & Steen, G. O. (1974) *Eur. J. Biochem. 46*, 243−258.
Kates, M. (1986) *Techniques in Lipidology*, 2nd ed., pp 102−108, 110−111, 172−175, 186−197, 232−242, 254−278, and 370, Elsevier, New York.
Kornblatt, M. J. (1979) *Can. J. Biochem. 57*, 255−258.
Kornblatt, M. J., Knapp, A., Levine, M., Schachter, H., & Murray, R. K. (1974) *Can. J. Biochem. 52*, 689−697.
Law, H., Itkonnen, O., & Lingwood, C. A. (1988) *J. Cell. Physiol. 137*, 462−468.
Levine, M., Bain, J., Narasimhan, R., Palmer, B., Yates, A. J., & Murray, R. K. (1976) *Biochim. Biophys. Acta 441*, 134−145.
Lingwood, C. A. (1985) *Can. J. Biochem. Cell Biol. 63*, 1077−1085.
Lingwood, C. A. (1986) *Biochem. Cell Biol. 64*, 984−992.
Murray, R. K., & Narasimhan, R. (1990) in *Glycolipids, Phosphoglycolipids, and Sulfoglycolipids* (Kates, M., Ed.) pp 321−361, Plenum Press, New York.
Murray, R. K., Narasimhan, R., Levine, M., & Pinteric, L. (1980) in *Cell Surface Glycolipids*, ACS Symposium Series 128 (Sweeley, C. C., Ed.) pp 105−125, American Chemical Society, Washington, DC.
Parks, J. E., & Lynch, D. V. (1992) *Cryobiology 29*, 255−266.
Rogers, B. J., & Yanagimachi, R. (1976) *Biol. Reprod. 15*, 614−619.
Roldan, E. R. S., & Harrison, R. A. P. (1989) *Biochem. J. 259*, 397−406.
Ruknudin, A. (1989) *Gamete Res. 22*, 375−384.
Saling, P. M., Wolf, D. P., & Storey, B. T. (1978) *Dev. Biol. 65*, 515−525.
Siminovitch, D. J., Wong, P. T. T., & Mantsch, H. H. (1987a) *Biochim. Biophys. Acta 900*, 163−167.
Siminovitch, D. J., Wong, P. T. T., & Mantsch, H. H. (1987b) *Biophys. J. 51*, 465−473.
Stein, R. S., & Sutherland, G. B. B. M. (1953) *J. Chem. Phys. 21*, 370−371.
Stein, R. S., & Sutherland, G. B. B. M. (1954) *J. Chem. Phys. 22*, 1993−1999.
Stock, C. E., & Fraser, L. R. (1989) *J. Reprod. Fertil. 87*, 463−478.
Surewicz, W. K., Muga, A., & Mantsch, H. H. (1992) in *Structural and Dynamic Properties of Lipids and Membranes* (Quinn, P. J., & Cherry, R. J., Eds.) pp 153−164, Portland Press, Chapel Hill.
Suzuki, A., Ishizuka, I., Ueta, N., & Yamakawa, T. (1973). *Jpn. J. Exp. Med. 43*, 435−442.
Tanphaichitr, N., Smith, J., & Kates, M. (1990) *Biochem. Cell Biol. 68*, 528−535.
Tanphaichitr, N., Tayabali, A., Gradil, C., Juneja, S., Leveille, M. C., & Lingwood, C. A. (1992) *Mol. Reprod. Dev. 32*, 17−22.
Tanphaichitr, N., Smith, J., Mongkolsirikieart, S., Gradil, C., & Lingwood, C. A. (1993) *Dev. Biol. 156*, 164−175.
Tupper, S., Wong, P. T. T., & Tanphaichitr, N. (1992) *Biochemistry 31*, 11902−11907.
Vishunubhatla, I., Morris, K., & Adams, G. A. (1988) *Lipids 23*, 609−614.
Wolf, D., Hagopian, S. Jt., & Ishijima, S. (1986) *J. Cell. Biol. 102*, 1372−1377.
Wong, P. T. T. (1984) *Annu. Rev. Biophys. Bioeng. 13*, 1−24.
Wong, P. T. T. (1987) in *High Pressure Chemistry and Biochemistry* (van Eldik, R., & Jonas, J., Eds.) pp 381−400, D. Reidel Publishing Co., Boston.
Wong, P. T. T., & Mantsch, H. H. (1984) *J. Chem. Phys. 81*, 6367−6370.
Wong, P. T. T., & Mantsch, H. H. (1985) *J. Chem. Phys. 83*, 3268−3275.
Wong, P. T. T., & Mantsch, H. H. (1988) *Chem. Phys. Lipid 46*, 213−224.
Wong, P. T. T., Moffat, D. J., & Baudais, F. L. (1985) *Appl. Spectrosc. 39*, 733−735.
Wong, P. T. T., Siminovitch, D. J., & Mantsch, H. H. (1988) *Biochim. Biophys. Acta 947*, 139−171.
Yanagimachi, R. (1994) in *The Physiology of Reproduction* (Knobil, E., & Neill, J. D., Eds.) pp 189−317, Raven Press, New York.
Yanagimachi, R., & Usui, N. (1974) *J. Biochem. (Tokyo) 52*, 226−227.